

Supporting Information for:

Photo-Assisted Electrodeposition of MoS₂ from Ionic Liquid on Organic-Functionalized Silicon Photoelectrodes for H₂ Generation

Daniel Redman,[†] Hark Jin Kim,[†] Keith J. Stevenson*
and Michael J. Rose*

Department of Chemistry, The University of Texas at Austin, Austin, TX 78712, United States

Table of Contents

Figure S1: Water contact angle measurements of organic modified *p*-Si(111) substrates.

Figure S2: XPS spectra of the Si 2p and C 1s of regions of the *p*-Si(111)|diOMe substrate.

Figure S3: EIS measurements of the organic-modified *p*-Si(111) substrate with 5 mM ethyl viologen in 0.1 M LiClO₄/MeCN. EIS measurements of *p*-Si(111)|CH₃ substrate in 0.5 M H₂SO₄.

Figure S4: First scan of CV and DCVA of FTO in [MoS₄]²⁻ – EMIM-TFSI electrolyte in the absence and presence of [PipH][TFSI].

Figure S5: Effect of light on open circuit potential of organic-coated *p*-Si(111), anodic stability of bare *p*-Si(111) in ionic liquid electrolyte, and CV deposition of MoS_x on *p*-Si(111)|Ph.

Figure S6: Survey spectra of MoS_x on organic-coated *p*-Si(111) electrodes and high resolution XPS spectra of Mo 3d and S 2p of *p*-Si(111)|Ph|MoS_x.

Figure S7: Raman spectra of electrodeposited MoS_x on organic-coated *p*-Si(111) and glassy carbon.

Figure S8. Atomic force microscopy height retraces for MoS_x on organic-coated *p*-Si(111).

Figure S9: PEC-HER test of *p*-Si(111)|H|MoS_x

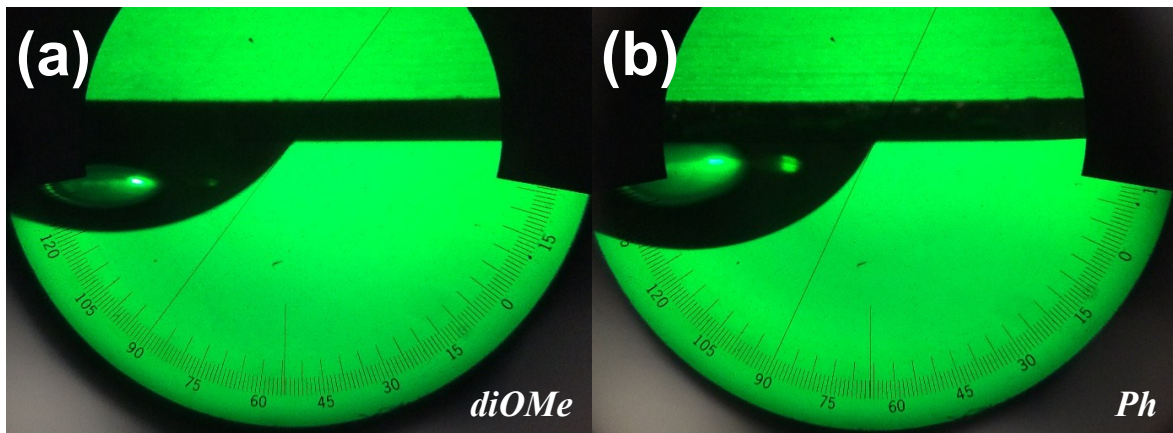


Figure S1. Water contact angle of (a) $p\text{-Si}(111)\text{|diOMe}$ and (b) $p\text{-Si}(111)\text{|Ph}$ surfaces with a 10 μL water drop.

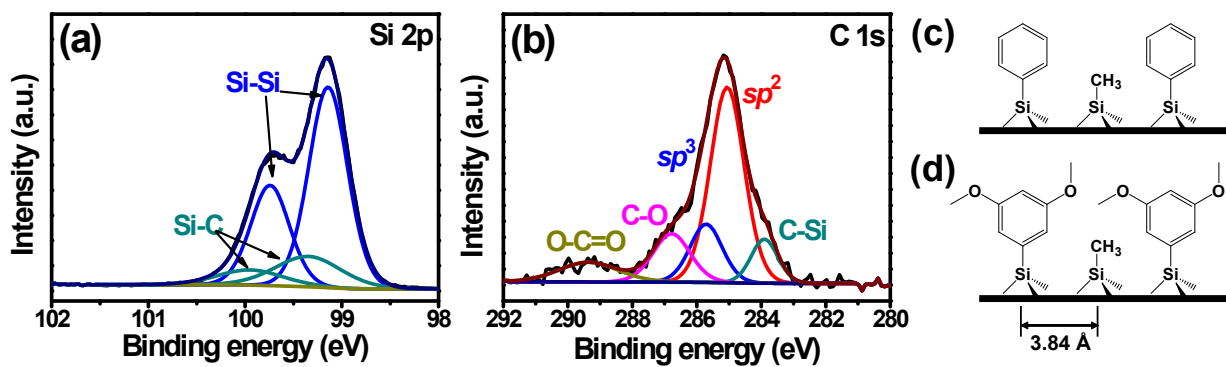


Figure S2. X-ray photoelectron spectrum of (a) Si 2p and (b) C 1s for $p\text{-Si}(111)\text{|diOMe}$ surface, and depiction of organic molecules attached to Si(111) for (c) $p\text{-Si}(111)\text{|Ph}$ and (d) $p\text{-Si}(111)\text{|diOMe}$.

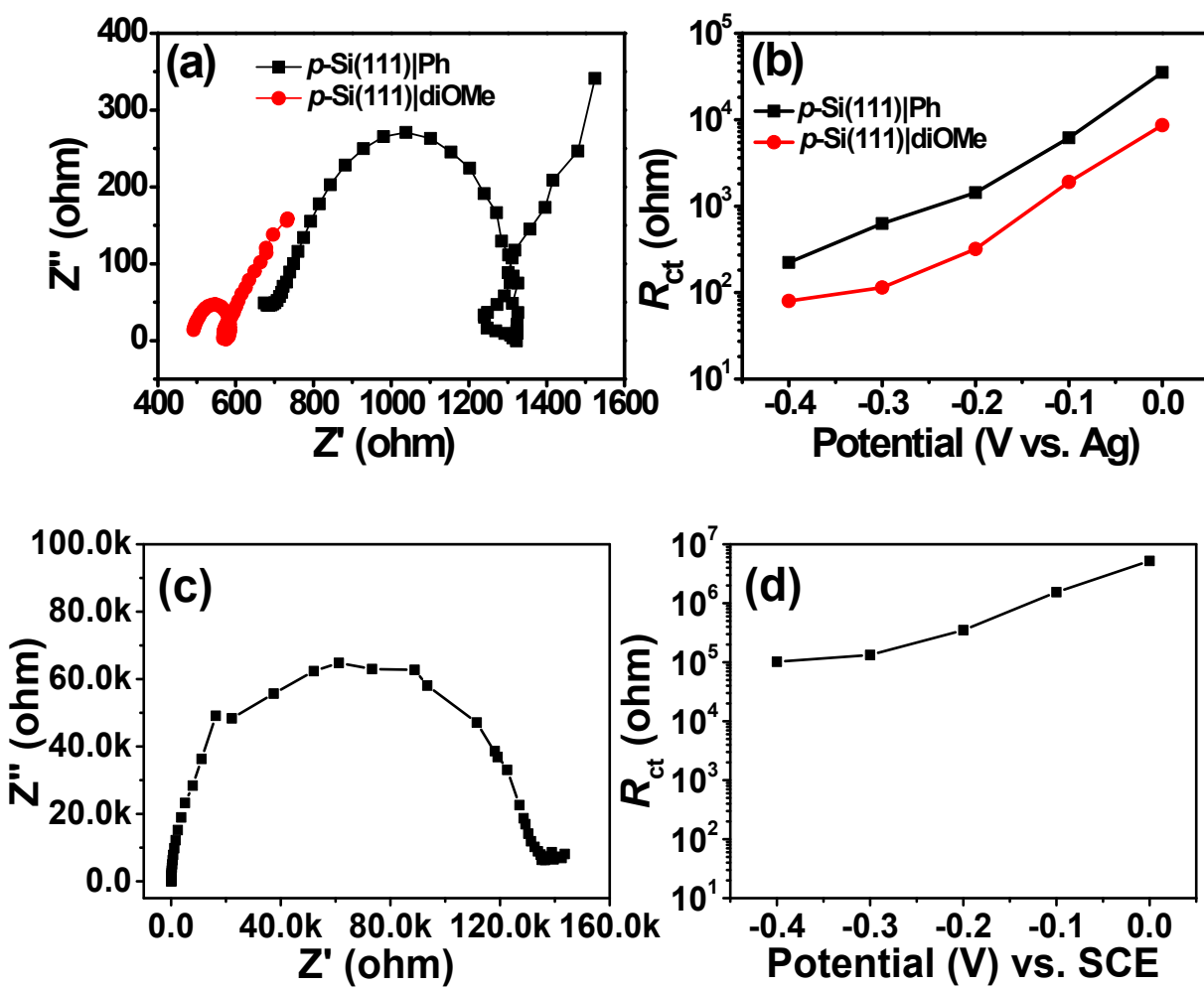


Figure S3. (a) Nyquist plots for $p\text{-Si}(111)|\text{Ph}$ (black) and $p\text{-Si}(111)|\text{diOMe}$ (red) surfaces. (b) Representation of the different resistances determined by EIS and plotted versus the applied potential. Conditions: Ag-wire reference electrode, 5 mM ethyl viologen in 0.1 M LiClO₄/MeCN, 1-sun irradiation, 10 mV AC amplitude, $10^5 < f < 0.1$ Hz. (c) Nyquist Plot for $p\text{-Si}(111)|\text{CH}_3$ at $E = -0.3$ V vs. SCE. (d) Potential dependence of charge transfer resistance of $p\text{-Si}(111)|\text{CH}_3$ as determined by EIS. Conditions: 0.5 M H₂SO₄, 1-sun irradiation, 10 mV AC amplitude, frequency range $10^5 < f < 0.1$ Hz.

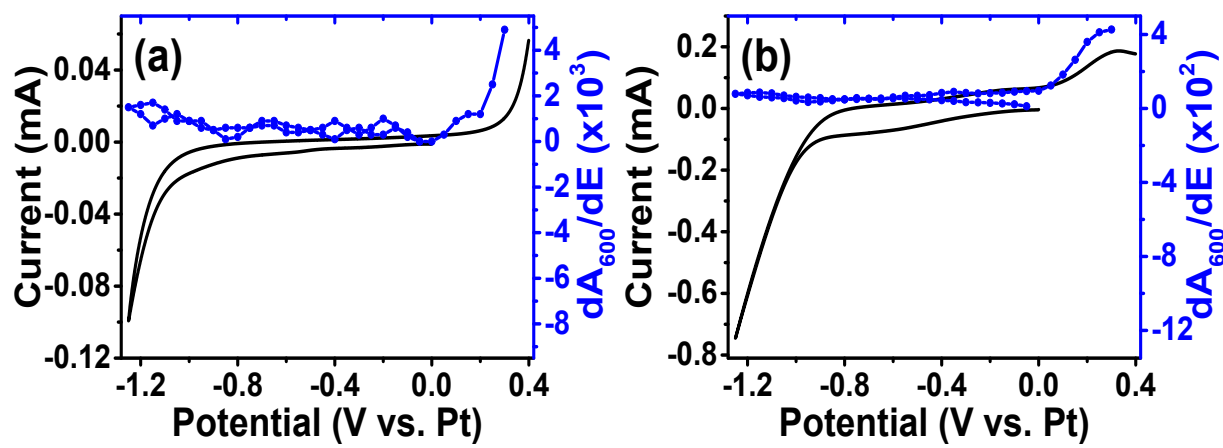


Figure S4. First scan of cyclic voltammogram and derivative cyclic voltabsorptometry of 0.005 M $[\text{MePipH}]_2[\text{MoS}_4]$ in the (a) absence and (b) presence of 0.2 M $[\text{PipH}][\text{TFSI}]$, $\lambda = 600$ nm, scan rate = 50 mV/s.

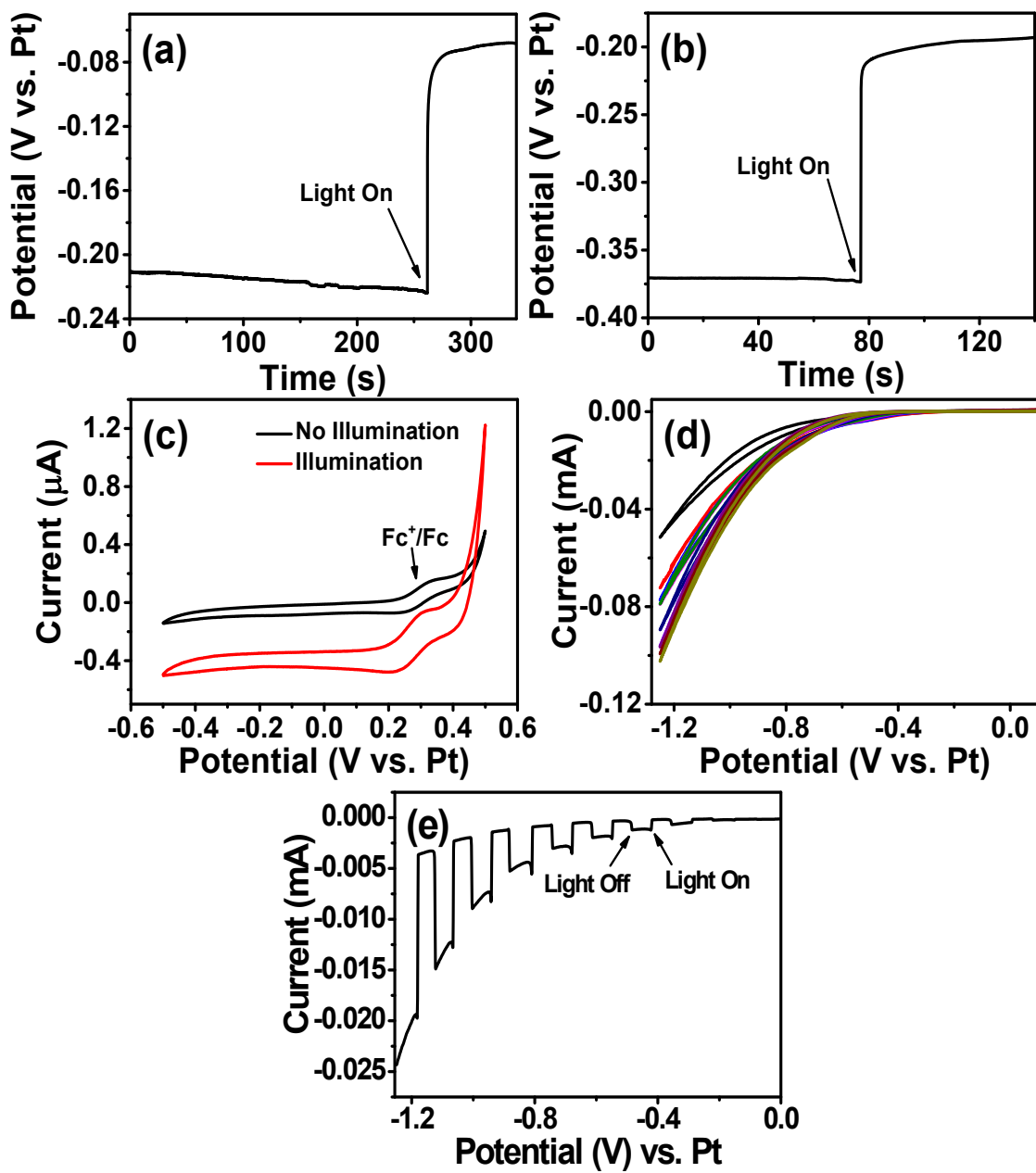


Figure S5. Effect of LED light on the open circuit potential of (a) *p*-Si|diOMe and (b) *p*-Si(111)|Ph with 0.005 M [MePipH]₂[MoS₄] and 0.2 M [PipH][TFSI] in EMIM-TFSI. (c) Cyclic voltammogram depicting anodic stability of bare *p*-Si(111) in 0.002 M ferrocene in EMIM-TFSI. (d) CV deposition of MoS_x on *p*-Si(111)|Ph and (e) first scan of the CV deposition on *p*-Si(111)|Ph with alternating light on and off with 0.005 M [MePipH]₂[MoS₄] and 0.2 M [PipH][TFSI] in EMIM-TFSI, scans 1-5, 10, 20, 30, 40, 50. Scan rate = 50 mV/s.

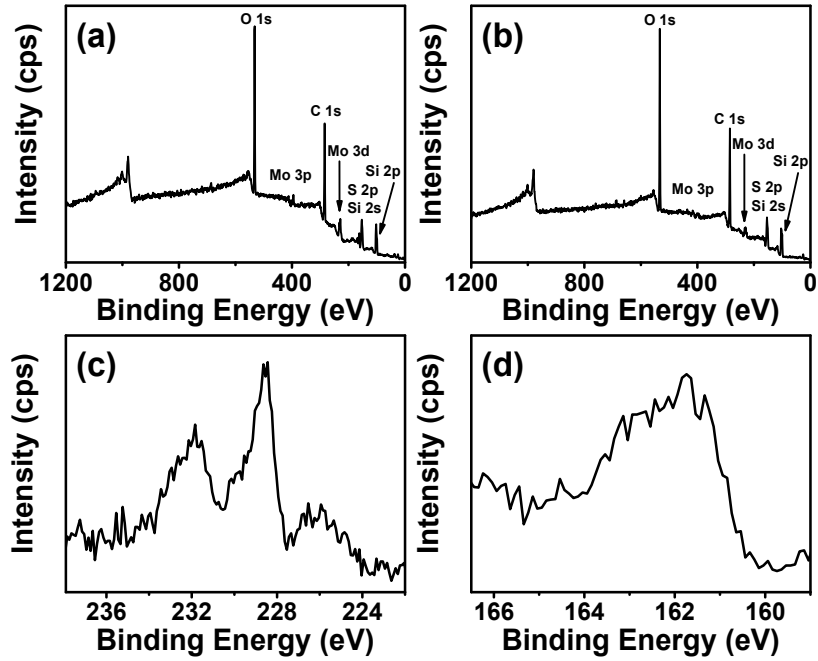


Figure S6. XPS survey spectra of (a) $p\text{-Si}(111)|\text{diOMe}|\text{MoS}_x$ and (b) $p\text{-Si}(111)|\text{Ph}|\text{MoS}_x$. High resolution XPS spectrum of (c) Mo 3d and (d) S 2p regions of $p\text{-Si}(111)|\text{Ph}|\text{MoS}_x$.

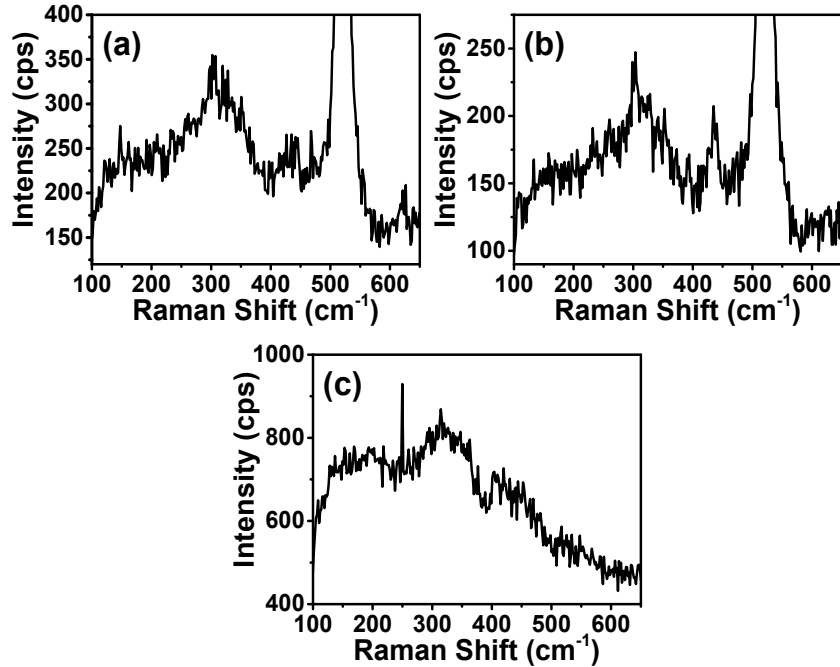


Figure S7. Raman spectra of (a) $p\text{-Si}(111)|\text{diOMe}|\text{MoS}_x$, (b) $p\text{-Si}(111)|\text{Ph}|\text{MoS}_x$, and (c) $\text{GC}|\text{MoS}_x$.

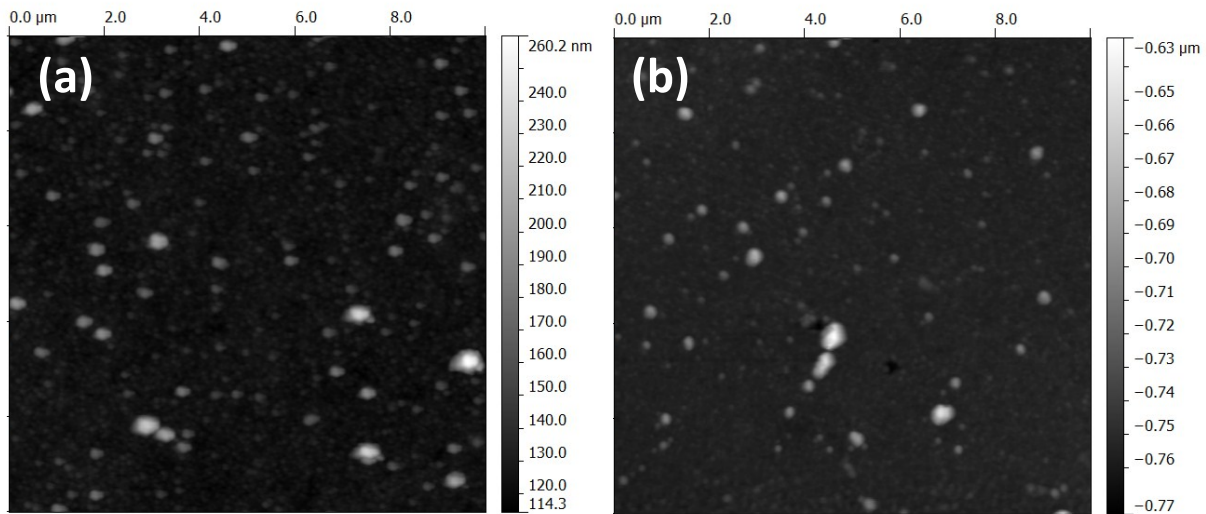


Figure S8. Atomic force microscopy height retraces of (a) $p\text{-Si}(111)\text{|diOMe|MoS}_x$ and (b) $p\text{-Si}(111)\text{|Ph|MoS}_x$.

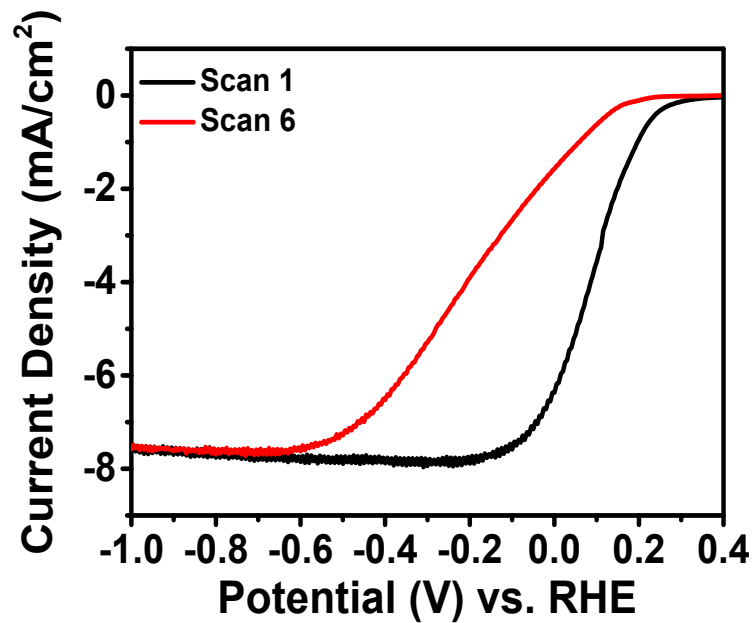


Figure S9: PEC-HER test of $p\text{-Si}(111)\text{|H|MoS}_x$ in 0.5 M H_2SO_4 (1-sun irradiation, scan rate = 100 mV/s), indicating instability of the hydride-terminated surface during catalytic conditions.